

Original Article

Effects of stellate ganglion block on inflammation and autophagy of spinal cord neurons in rats with neuropathic pain after spinal cord injury

Yuanxin Huang^{1*}, Hai Xu^{2*}, Dongmei Mao¹, Jinqi Shao³, Lili Deng⁴, Tingyu Wang⁵, Zeqing Liao⁶, Xue Li⁷, Yutao Chen⁷, Jing Yao¹, Zhongjie Zhang¹

¹Department of Pain, The Affiliated Hospital of Guizhou Medical University, Guiyang 550004, Guizhou, China;

²College of Anesthesiology, Guizhou Medical University, Guiyang 550004, Guizhou, China; ³Department of Anesthesiology, The Affiliated Hospital of Guizhou Medical University, Guiyang 550004, Guizhou, China;

⁴Department of Anesthesiology, Guiyang Baiyun District People's Hospital, Guiyang 550004, Guizhou, China;

⁵Department of Anesthesiology, Jiangjin Hospital Affiliated to Chongqing University, Chongqing 402260, China;

⁶Department of Anesthesiology, Guizhou Provincial People's Hospital, Guiyang 550002, Guizhou, China; ⁷College of Anesthesiology, Guizhou Medical University, Guiyang 550004, Guizhou, China. *Equal contributors and co-first authors.

Received November 26, 2024; Accepted April 1, 2025; Epub April 15, 2025; Published April 30, 2025

Abstract: Objective: To assess the therapeutic effects of stellate ganglion block (SGB) on spinal cord injury (SCI)-induced neuropathic pain in rats, and to explore its potential mechanisms in alleviating neuropathic pain, thereby providing a theoretical foundation for clinical treatment. Methods: A rat model of SCI was established, and animals were randomly assigned to one of three groups: the sham surgery group (Sham), the SCI group (SCI), or the SCI group treated with SGB (SCI + SGB). Motor function was assessed using the Basso Beattie Bresnahan (BBB) locomotor rating scale, while thermal hyperalgesia was evaluated using hot plate test. Enzyme-linked immunosorbent assay (ELISA) was utilized to measure the levels of inflammatory cytokines, including interleukin-1 β (IL-1 β), IL-6, and tumor necrosis factor- α (TNF- α), within the spinal cord. Hematoxylin-eosin (HE) staining was performed to observe spinal cord histopathology. Terminal deoxynucleotidyl transferase-mediated dUTP nick-end labeling (TUNEL) staining was used to detect apoptotic cells, and transmission electron microscopy was employed to visualize autophagosomes. Expression of autophagy-related proteins LC3-II/LC3-I and p62 was examined via Western blotting. Results: Compared with the sham group, rats in the SCI group displayed impaired hind limb motor function, decreased pain thresholds, elevated inflammatory cytokine levels, significant spinal cord pathology, increased apoptosis, altered expression of autophagy-related protein, and disrupted autophagic flux. In contrast, SGB treatment improved motor function, alleviated pain, reduced inflammatory cytokines levels, mitigated spinal cord injury and apoptosis, and enhanced autophagy with improved autophagic flux. Conclusions: Stellate ganglion block alleviates neuropathic pain in SCI-induced rats by reducing pro-inflammatory cytokine levels, mitigating spinal cord apoptosis and injury, promoting autophagy, and restoring autophagic flux in the spinal cord.

Keywords: Stellate ganglion block, neuropathic pain, spinal cord injury

Introduction

Spinal cord injury (SCI) is a severe form of central nervous system damage, affecting an estimated 40 to 80 million people globally each year [1]. Owing to the challenges associated with treatment and the generally poor prognosis, SCI remains a significant global public health concern. Neuropathic pain following SCI is well-documented [2]. A study reported that

pain is a predominant issue among individuals with traumatic SCI, with a substantial prevalence rate of 77% reported among the affected population [3]. Although the exact mechanisms underlying SCI-induced pain remain unclear, research suggests that neurophysiological changes in the spinal cord and peripheral nervous system contribute to its development [4, 5]. Persistent pain is typically associated with increase neuronal excitability and gliosis in the

central nervous system, both of which are common sequelae of nerve trauma [6, 7]. Secondary injury following SCI is characterized by inflammation, cell death, and glial scar formation, all of which hinder recovery. Consequently, targeting these pathological processes may offer a potential treatment strategy for SCI [8].

Stellate ganglion block (SGB) is a well-established and effective approach for temporarily blocking the cervical sympathetic trunk. Previous research indicated that SGB significantly improves patient outcomes in cerebrovascular diseases by mitigating cerebral vasospasms, augmenting cerebral oxygenation, diminishing inflammatory responses, and attenuating oxidative stress through multiple mechanisms. Recently, SGB has demonstrated promising potential in pain management, notably in alleviating complex regional pain syndrome, postoperative pain, and orofacial pain [9-12]. However, the application of SGB in neuropathic pain following SCI remains largely unexplored.

The mechanisms through which SGB modulates neuroinflammation and autophagy in central spinal pain following SCI remain unclear. We speculate that SGB may alleviate neuropathic pain by modulating neuroinflammation and autophagy in the spinal cord's dorsal horn. Investigating the underlying mechanisms of SGB in post-SCI neuropathic pain could bridge a critical research gap and provide a theoretical basis for the development of novel therapeutic approaches. Confirming the effectiveness of SGB in alleviating neuropathic pain after SCI could pave the way for new clinical strategies, improving patient outcomes, reducing distress, and advancing treatment modalities. Thus, this study aims to comprehensively evaluate the effects of SGB on spinal cord inflammation and autophagy in a rat model with post-SCI neuropathic pain, establishing a robust foundation for subsequent research and clinical applications.

Materials and methods

Animals

Adult male Wistar rats weighing between 200-250 g were purchased from the Experimental Animal Center of Guizhou Medical University (Guiyang, China). The rats were housed in a temperature- and humidity-controlled environ-

ment under a 12-hour light/dark cycle with ad libitum access to water and food. The experimental protocol was approved by the Institutional Ethics Committee of the Affiliated Hospital of Guizhou Medical University. Rats were randomly divided into three groups: Sham (n = 42), SCI (n = 42), SCI + SGB (n = 42). The Sham group underwent a laminectomy without spinal cord injury. The SCI group was subjected to spinal cord injury to establish the SCI model. The SCI + SGB group received stellate ganglion block (SGB) following SCI.

Animal model of SCI

Before the procedure, rats were anesthetized with an intraperitoneal injection of pentobarbital sodium (50 mg/kg) and then placed in a prone position. A 2.5 cm median dorsal incision was made centered over the T10 vertebra. The lamina and spinous processes of T9-T11 were removed to expose the underlying dura mater. Hemostasis was ensured before applying a calibrated hemostatic clamp to compress the spinal cord for 40 seconds. Upon release, a bright red hematoma was observed on the dura mater at the compression site, confirming successful injury induction. Postoperatively, hemostasis, wound disinfection, and suturing were performed. Rats were kept warm under a heat lamp until spontaneous recovery. Bladder expression was conducted manually three times daily to assist with urination.

Stellate ganglion block

Ten minutes after spinal cord injury, rats in the SGB group underwent the SGB procedure. The neck was prepared by removing fur, and the median incision site was thoroughly cleaned and disinfected with iodophor. The connective tissue adjacent to the right side of the trachea was carefully dissected. Anatomical observations revealed the fusiform superior cervical ganglion dorsally at the bifurcation of the right common carotid artery, with a light-yellow structure approximately 3 mm inferior to it, identified as the cervical sympathetic nerve trunk (the right stellate ganglion). This structure was dissected at its proximal end, followed by wound disinfection and suturing. Successful block placement was confirmed by the appearance of typical Horner's syndrome upon regaining consciousness, characterized by per-

sistent right eyelid ptosis, pupil constriction, and narrowing of the palpebral fissure.

Behavior

Basso, beattie, and bresnahan (BBB) scoring: The Basso, Beattie, and Bresnahan (BBB) scoring system is a widely used method for evaluating hind limb motor function following SCI. Originally developed by Basso et al. [13], this system provides a comprehensive and reliable evaluation of locomotor recovery, with its validity and reliability well-established in numerous studies [14]. It remains the gold standard for motor function assessment in SCI research. Hind limb motor function recovery was evaluated using the BBB scoring system by two researchers blinded to this study. The BBB scale ranges from 0 (no movement) to 21 (normal movement). Evaluations were conducted before surgery and on post-injury days 1, 3, and 7. At each time point, two rats were evaluated, and their scores were recorded to calculate an average value.

Heat paw thermal withdrawal latencies (PWL): To evaluate thermal hyperalgesia, the hot plate test was used to assess the nociceptive response of the hind paw to noxious heat. The platform was heated to 55°C, and then rats were placed on the platform. The test was terminated when the animal exhibited paw withdrawal or licking behaviors, and the latency to these behaviors was recorded. The hot plate test is a widely used method for assessing nociceptive responses to thermal stimuli in rodents. It operates on the principle that animals reflexively withdraw their paws from a heated surface to avoid pain. Its reliability and validity have been well-demonstrated in previous studies [15].

Tissue preparation

At each designated time point, animals were anesthetized with an intraperitoneal injection of pentobarbital sodium (50 mg/kg). The spinal cord was sectioned into three parts for different analyses: 1. *Histological Staining:* A portion of the tissues was fixed in 4% paraformaldehyde (Sigma-Aldrich, USA) for 48 hours, dehydrated in 20% sucrose solution, and then cut into 10 µm cross-sections for HE and TUNEL staining. 2. *Transmission Electron Microscopy (TEM):* A small segment of the spinal cord (< 1

mm³) was fixed overnight in 2.5% glutaraldehyde phosphate buffer for TEM observation. 3. *Western Blot and ELISA:* Following intracardiac perfusion with 0.1 M PBS, another portion of spinal cord tissue was immediately excised and cut into 20 mm segments centered on the injury site on an ice-cold plate. The tissue was carefully shredded and homogenized in a buffer solution containing TRIzol reagent and 0.1% protease inhibitor (Beyotime Institute of Biotechnology, Jiangsu, China) for subsequent protein and RNA extraction. Samples were then frozen at -80°C for later analysis.

At the end of the experiment, after all experimental procedures were completed and tissue samples were collected, the rats were euthanized by a lethal dose of pentobarbital sodium (150 mg/kg, intraperitoneal injection) to ensure a painless and humane death. This euthanasia method adheres to ethical guidelines for animal research and is widely used in laboratory studies.

Hematoxylin and eosin (HE) staining

Tissues were first stained with hematoxylin for 45 seconds, followed by a 10-second rinse in distilled water. Differentiation was achieved by treating the tissues with a 1:100 HCl/95% alcohol solution for five seconds, followed by a 30-minute wash in water. The sections were then stained with eosin for 15 seconds, rinsed with water for 10 minutes, dehydrated, and mounted with neutral gum.

Enzyme-linked immunosorbent assay (ELISA)

Spinal cord specimens were placed in a homogenizer, and an appropriate volume of pre-cooled homogenization buffer containing protease inhibitors was added to prevent protein degradation. The tissue was homogenized on ice until fully disrupted. The homogenate was then transferred to a centrifuge tube and subjected to three freeze-thaw cycles (freezing in liquid nitrogen and thawing in a 37°C water bath) to further disrupt cells and release inflammatory factors. Next, the homogenate was centrifuged at 4°C and 10,000 g for 10 minutes, and the supernatant was carefully collected for analysis. An ELISA kit from Beyotime (Wuhan, China) was utilized, following the manufacturer's instructions. A standard curve was generated by performing gradient dilutions of

the standards and adding them to the standard wells of the microplate. Samples were loaded into their respective sample wells, with each sample tested in duplicate. The plate was then incubated at room temperature for a specified duration according to the kit instructions, allowing the inflammatory factors to bind to the antibodies coated on the microplate. Following incubation, the microplate was washed multiple times with the provided wash solution to remove unbound substances. The enzyme-labeled secondary antibody was then added, followed by another incubation at room temperature, allowing the secondary antibody to bind specifically to the primary antibody attached to the inflammatory factors. After a final wash, a chromogenic substrate was added and incubated in the dark to develop the color reaction. Absorbance values were measured at 450 nm and 550 nm using a microplate reader. The concentrations of IL-1 β , IL-6, and TNF- α in the samples were calculated based on the standard curve, with results expressed in pg/mg protein.

Transmission electron microscope

Samples were fixed with osmic acid and then dehydrated through a graded alcohol series before being sectioned into ultrathin slices (70-90 nm). The slices were then stained for 15 minutes with lead citrate and a 50% ethanol-saturated uranyl acetate solution. The autophagic structures were then observed using TEM (JEM-1011, JEOL, Japan).

TUNEL staining

TUNEL staining was used to label and quantify apoptotic cells. Slices were processed using an *in situ* cell death detection kit (Roche Mannheim, Germany) according to the manufacturer's instructions. DNase free proteinase K (Solarbio, Beijing, China) was diluted in 10 mM Tris HCl solution to a working concentration of 20 μ g/ml. Then, the slices were incubated for 20 minutes. After washing with PBS, the slices were treated with TUNEL detection solution and incubated in the dark at 37°C for 1 hour. Following another PBS wash, the slices were counterstained with DAPI and examined under a fluorescence microscope (IX71, Olympus, Tokyo, Japan). Five fields of view were selected per sample, and the average number of labeled apoptotic cells was quantitatively analyzed.

Western blotting

Protein concentrations were determined using the Bradford assay. Equal amounts of protein were separated via 10% SDS-PAGE and transferred onto a PVDF membrane. The membrane was blocked with 5% skim milk at room temperature for 60 minutes, followed by incubation at 4°C for 12 hours with primary antibodies targeting LC3-II (mouse, 1:500), LC3-I (mouse, 1:100), p62 (rabbit, 1:1000), and GAPDH (mouse, 1:15000) (all sourced from Beyotime, Wuhan, China). After washing with TBST, the membrane was incubated at room temperature for 60 minutes with HRP-conjugated goat anti mouse (1:5000), or goat anti rabbit (1:5000) secondary antibodies (Bayotai, Wuhan, China). Immunolabeled protein bands were detected using an enhanced chemiluminescence kit, and grayscale analysis was performed using ImageJ software.

Statistical analysis

Data were expressed as mean \pm Standard Error of the Mean (SEM). Statistical analysis was performed using GraphPad Prism version 8.0. A non-paired student's t-test was used for comparisons between the two groups. For multiple-group comparisons, one-way, two-way, or repeated measures ANOVA followed by the Newman-Keuls test was applied. A *P*-value < 0.05 was considered statistically significant.

Results

SGB promoted functional recovery after SCI

The BBB results showed that the sham surgery group maintained full hind limb motor function at all observation time points (6 h, 12 h, 24 h, 48 h, 5 d, 7 d, and 14 d post-injury). In the SCI group, motor function gradually improved over time but remained significantly impaired compared to the sham group (*P* < 0.05). At each evaluation time point, the SCI + SGB group exhibited greater motor function recovery compared to the SCI group (all *P* < 0.01), indicating that SGB promotes functional recovery after SCI (*P* < 0.05) (**Figure 1**).

SGB alleviated neuropathic pain in rats after SCI

Paw withdrawal latency (PWL) was utilized to quantify neuropathic pain in rats. On days 5, 7,

SGB Alleviates NP

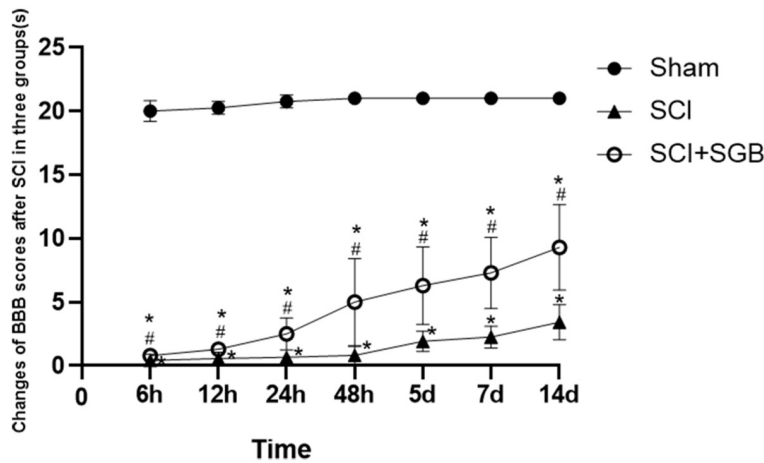


Figure 1. BBB scoring system evaluation of hind limb motor function in rats with spinal cord injury. Mean \pm Standard Error of the Mean (SEM) describes the data. $n = 42$. Compared with the sham surgery group, meeting the criteria of $P < 0.05$, represented by *. Compared with the spinal cord injury (SCI) group, meeting the criteria of $P < 0.05$, represented by #.

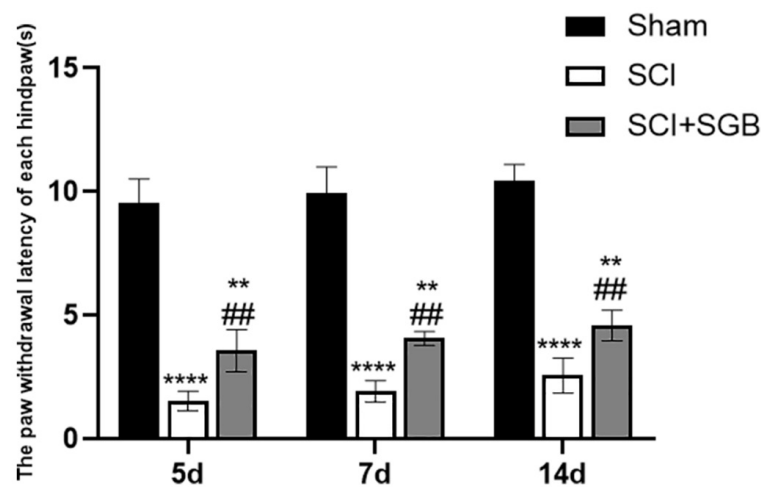


Figure 2. Schematic diagram of using paw thermal withdrawal latencies (PWL) to quantify pain related content in rats. Mean \pm Standard Error of the Mean (SEM) describes the data. $n = 42$. Compared with the sham surgery group, meeting the criteria of $P < 0.01$, represented by **, meeting the criteria of $P < 0.0001$, represented by ****. Compared with the spinal cord injury (SCI) surgery group, meeting the criteria of $P < 0.01$, represented by ##.

and 14 post-SCI, no significant changes in PWL values were observed in the sham surgery group, whereas both the SCI and SCI + SGB groups exhibited significantly reduced PWL values ($P < 0.01$), indicating the presence of neuropathic pain. However, compared to the SCI group, the SCI + SGB group demonstrated significantly increased PWL values ($P < 0.05$), suggesting that SGB alleviated neuropathic pain after SCI (Figure 2).

SGB reduced the levels of IL-1 β , IL-6, and TNF- α in the spinal cord tissue of rats after SCI

At 1, 3, and 7 days post-injury, inflammatory factor levels in the sham group remained stable. In contrast, IL-1 β , IL-6, and TNF- α levels were significantly elevated in the SCI group compared to the sham group at all observed time points (all $P < 0.05$). However, the SCI + SGB group exhibited significantly lower levels of IL-1 β , IL-6, and TNF- α compared to the SCI group at all three time points (all $P < 0.05$) (Figure 3).

SGB alleviated spinal cord injury in SCI rats

Hematoxylin and eosin (HE) staining revealed no hemorrhagic necrosis or tissue edema in the spinal cord of the sham group. At 1-day post-injury, both the SCI and SCI + SGB groups exhibited indistinct boundaries between gray and white matter at the injury site, with patchy hemorrhage, tissue edema, and nuclear pyknosis in the gray matter. However, no significant differences were observed between the SCI + SGB and SCI groups at this time point. At 14 days post-injury, the SCI group exhibited prominent necrotic cystic cavities within the spinal cord tissue and white matter.

In contrast, the SCI + SGB group exhibited smaller cystic cavities, suggesting that SGB mitigated spinal cord damage following SCI (Figure 4).

SGB inhibited apoptosis of spinal cord cells induced by SCI

TUNEL staining was employed to detect apoptosis levels in spinal cord tissue. Seven days

SGB Alleviates NP

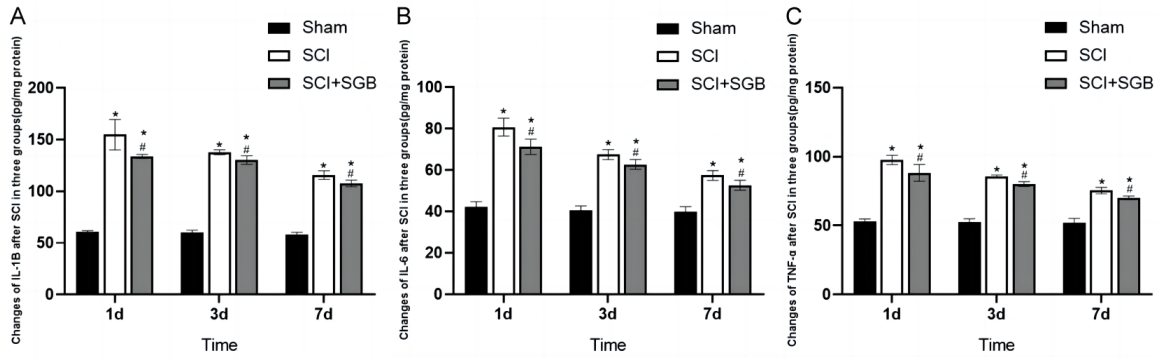


Figure 3. Stellate ganglion block (SGB) reduces the levels of IL-1 β and other factors in the spinal cord of rats after spinal cord injury. A: Used enzyme-linked immunosorbent assay (ELISA) to evaluate the levels of interleukin-1 β (IL-1 β) in spinal cord samples from different groups. B: Used ELISA to evaluate the levels of interleukin-6 (IL-6) in spinal cord samples from different groups. C: Evaluate the levels of tumor necrosis factor- α (TNF- α) in spinal cord samples from different groups using ELISA. Mean \pm Standard Error of the Mean (SEM) describes the data. n = 42. Compared with the sham group, meeting the criteria of P < 0.05, represented by *. Compared with the spinal cord injury (SCI) group, meeting the criteria of P < 0.05, represented by #.

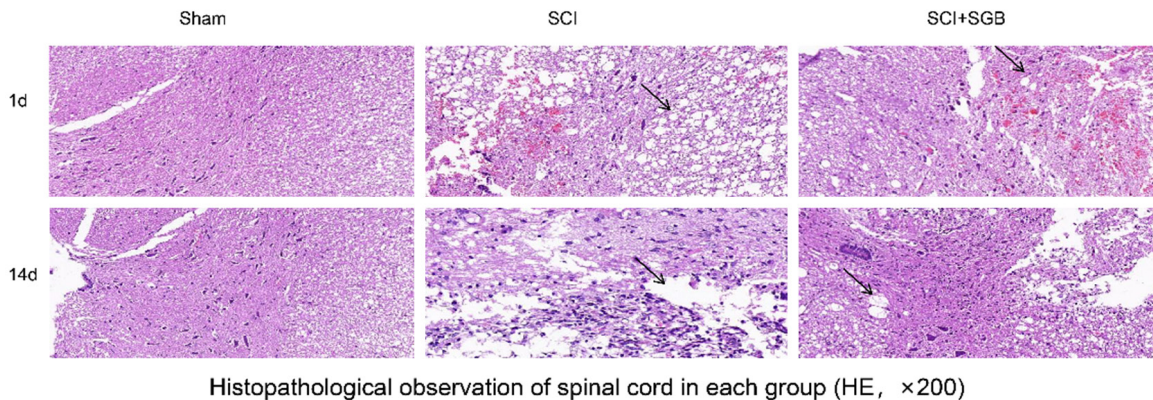


Figure 4. Histopathological observation of spinal cord tissue in each group.

post-injury, both SCI and SCI + SGB groups showed significantly higher levels of spinal cord cell apoptosis compared to the sham surgery group (P < 0.001). Furthermore, compared with the SCI group, the SCI + SGB group exhibited significantly lower levels of spinal cord neuronal apoptosis (P < 0.01) (**Figure 5**).

SGB promoted spinal cord autophagy in SCI rats

TEM was applied to observe the microautophagosomes in spinal cord tissue at 7 days post-injury. The SCI group displayed incomplete mitochondrial structure, notable mitochondrial vacuolation, and disrupted myelin lamellar compared to the sham group, along with a limited number of autophagosomes. In contrast,

the SCI + SGB group displayed intact mitochondrial structures and a substantial increase in the number of autophagosomes (**Figure 6**), suggesting enhanced autophagic activity.

In this study, Western Blot analysis was utilized to quantitatively evaluate the levels of autophagy-related proteins across different groups. Compared with the sham surgery group, SCI group exhibited a significant upregulation in the levels of LC3-II/LC3-I and p62 proteins at all time points (all P < 0.05). Furthermore, the SCI + SGB group demonstrated a notable increase in LC3-II/LC3-I protein levels and a marked decrease in p62 expression compared to the SCI group (all P < 0.05). These findings suggest that SGB treatment enhances autophagic activity in SCI rats (**Figure 7A, 7B**).

SGB Alleviates NP

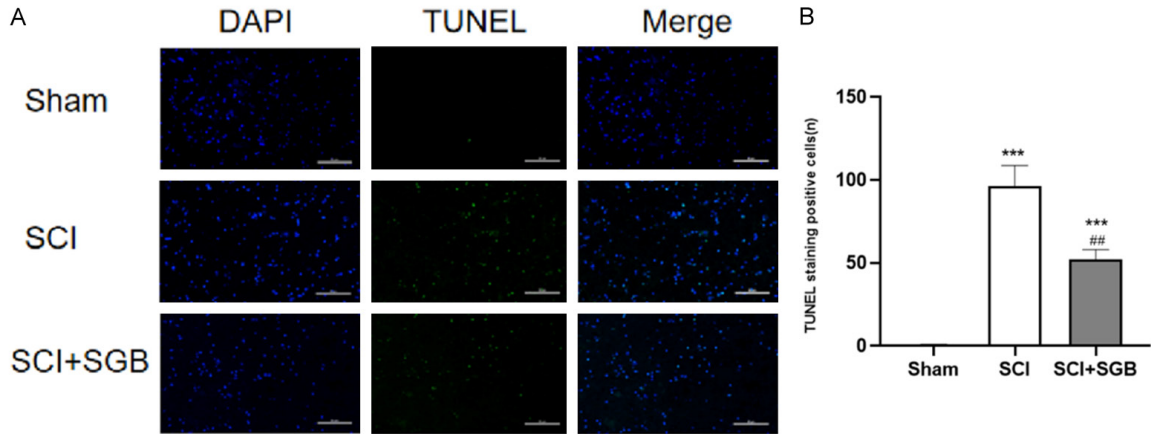


Figure 5. Stellate ganglion block (SGB) can inhibit apoptosis of spinal cord cells induced by SCI. A: Terminal deoxynucleotidyl transferase-mediated dUTP nick-end labeling (TUNEL) staining was employed to assess the levels of apoptosis in hippocampal tissues across different groups of rats, $\times 100$. B: Quantitative analysis of TUNEL-positive cells was conducted. Data: Mean \pm Standard Error of the Mean (SEM). $n = 42$. *** $P < 0.001$ vs Sham group. ## $P < 0.01$ vs spinal cord injury (SCI) group.

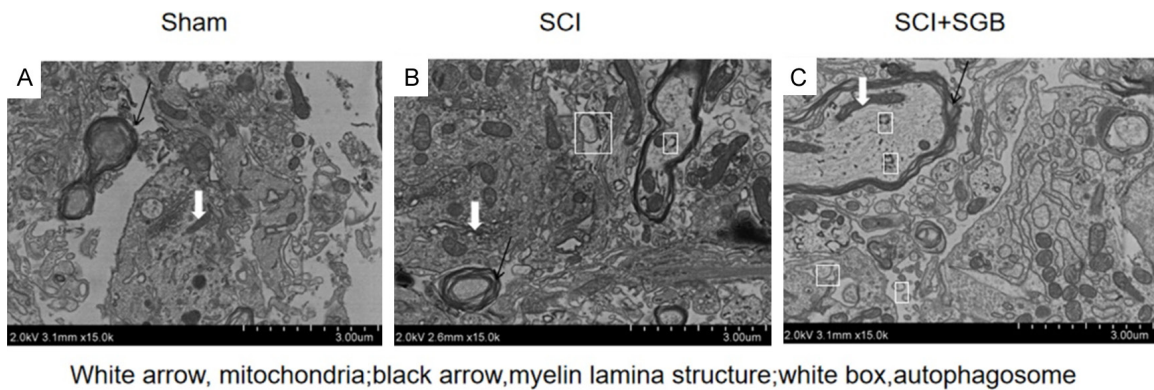


Figure 6. Changes of microautophagosomes in the rat spinal cord seven days after injury using transmission electron microscopy. A: Sham group. B: SCI group. C: SCI + SGB group.

Discussion

Chronic pain is a common complication following traumatic spinal cord injury (SCI) due to maladaptive neurophysiological and neurochemical changes in the somatosensory system [5, 16]. Currently, there is no effective way to treat chronic pain after SCI. SCI induces maladaptive changes in nociceptive synaptic circuits within the damaged spinal cord, which can also extend to remote areas, such as the limbic system and brainstem. These maladaptive nociceptive synaptic circuits can contribute to neuronal hyperexcitability and increased nociceptive transmission, leading to chronic central nervous system pain following SCI [16]. Yang et al. [17] reported that in humans, microglia

begin to release inflammatory factors such as IL-6 within 30 minutes of spinal cord injury. Green-Fulgham et al. [18] constructed a rat model of spinal cord contusion and found that administering an IL-1 receptor antagonists 72 hours post-injury significantly reduced apoptosis levels. These findings suggest that microglia play a key role in secondary injury by releasing inflammatory cytokines following SCI. The results of this study further confirm that inflammatory factor levels increase significantly after SCI, contributing to secondary injury and impairing sensory and motor recovery.

Further research is needed to develop effective treatments for neuropathic pain (NP) after SCI, as NP remains resistant to many pharmacologi-

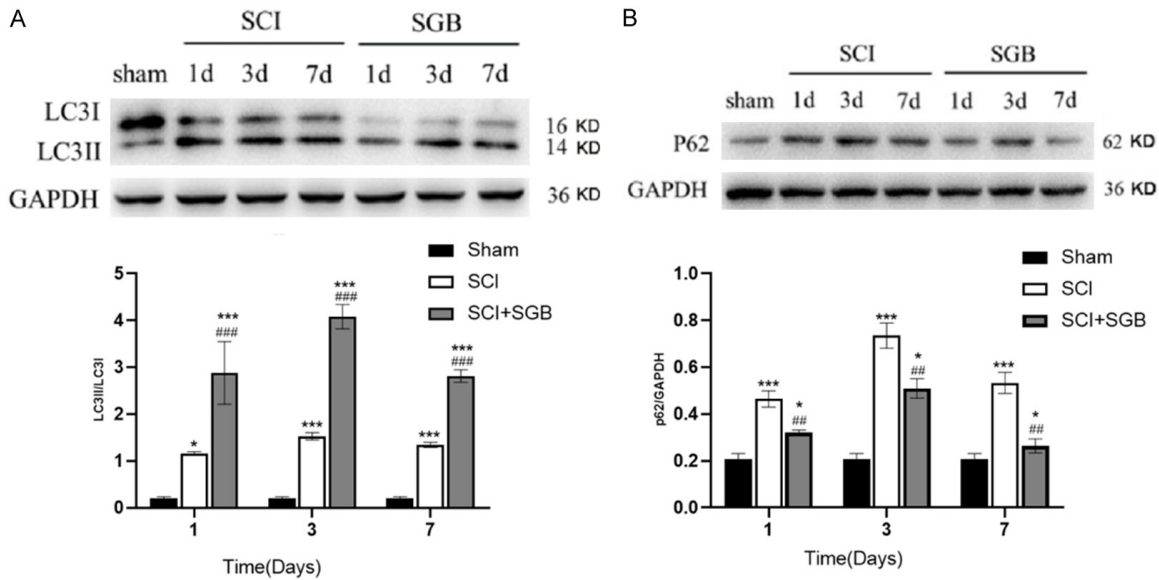


Figure 7. Stellate ganglion block (SGB) enhances autophagy in the spinal cords of rats with SCI. A: Western Blot analysis was used to determine the levels of Microtubule-associated protein 1 light chain 3 (LC3)-II/LC3-I proteins in spinal cord tissues across different groups of rats. B: Western Blot analysis was used to determine the levels of P62 protein in spinal cord tissues across different groups of rats. Data: Mean \pm Standard Error of the Mean (SEM). n = 42. * $P < 0.05$, *** $P < 0.001$ vs Sham group. ## $P < 0.01$, ### $P < 0.001$ vs spinal cord injury (SCI) group.

cal interventions [19, 20]. Although certain drugs have demonstrated efficacy, their therapeutic effects are often accompanied by adverse side effects, and treatment becomes more complex once SCI-related pain becomes chronic. Enhancing traditional pharmacological interventions or replacing them with nonpharmacological interventions has emerged as a promising approach to improving NP prognosis [21, 22]. However, the mechanisms underlying nonpharmacological interventions remain inadequately explored, limiting the development of effective treatments.

Since the 1940s, stellate ganglion block (SGB) has been used to treat sympathetically mediated pain [23]. This procedure involves local anesthesia of the stellate ganglion and its surrounding area to temporarily inhibit its function. In this study, SCI rats exhibited a significant reduction in pain threshold, whereas SGB elevated the pain threshold and alleviated pain. NP following SCI arises from multiple factors, including neuroinflammation, overactivity of spinal sensory neurons, activation of glial cells, abnormal synaptic transmission, and disturbance of the downstream regulatory systems. However, the precise mechanisms underlying NP remain unclear [2]. Recent studies

have shown that the spinal dorsal horn plays a key role in central sensitization and neuropathic pain development [2]. After peripheral nerve injury, pro-inflammatory cytokines activated in the spinal dorsal horn trigger the release of multiple inflammatory mediators, enhance the sensitivity of nociceptors, and contribute to NP progression [24].

The results of this study indicated that inflammatory cytokine levels, including IL-1 β were significantly lower in the SGB-treated group compared to the SCI model group. Histopathological analysis further revealed a reduction in inflammatory changes within the spinal cord following SGB treatment, suggesting that SGB plays a role in modulating the inflammatory response after SCI. The “vague-cholinergic anti-inflammatory pathway”, first described by Borovikova et al. [25], was evidenced in a lipopolysaccharide (LPS)-induced animal model, where acetylcholine inhibited inflammatory mediator release. This study provides further evidence that vagus nerve activity is integral to inflammation modulation following SCI. The autonomic nervous system comprises the sympathetic nervous system and the vagal nervous system, which interact to regulate physiological activities. Based on our experimental

results, we propose that the stellate ganglion, as the largest sympathetic ganglion in the body, may reflexively enhance vagal nerve activity when disrupted, thereby activating the “cholinergic anti-inflammatory pathway” to regulate post-SCI inflammation and reduce inflammatory factor levels in the spinal cord. Apoptosis plays a crucial role in tissue destruction and cellular stress, with its levels significantly increasing after SCI. Excessive apoptosis contributes to neuronal damage, leading to sensory and motor damage [26]. In this study, SGB was observed to decrease the level of apoptosis in the spinal cord, which may be key a mechanism by which SGB alleviates neuropathic pain after SCI.

Autophagy is a cellular self-protection mechanism activated in response to stress [27]. Macroautophagy, the most prevalent form, is regulated by ULK2 and the autophagy-associated Beclin-1/III PI3K complex. Upon activation, these complexes recruit key proteins involved in autophagosome formation and extension, including Atg12, Atg5, Atg16L, and LC3, resulting in the formation of conjugated complexes. LC3 binds to the phospholipid phosphatidylethanolamine to form LC3-II, which integrate into the autophagosome membrane, facilitating its extension and maturation. Autophagosomes subsequently fuse with lysosomes to form autolysosomes, where lysosomal enzymes degrade cellular components and damaged organelles [28, 29]. LC3-II interacts with P62 (also known as sequestosome-1, SQSTM1) and ubiquitinated protein aggregates, facilitating their engulfment in autophagosomes and regulating autophagy initiation and cell survival. Previous studies have demonstrated that elevated P62 levels are associated with impaired autophagic flux [30]. Li et al. [31] demonstrated increased expression of the autophagy marker protein Beclin-1 surrounding experimental SCI sites, with levels rising significantly within 4 hours post-injury, peaking on day 3, and persisting for up to 21 days. This suggests a correlation between central nervous system damage severity and autophagy biomarker levels, with prolonged autophagy activation potentially mitigating secondary injury [32]. Previous studies have shown that ischemic spinal cord injury enhances autophagy and promotes motor function recovery, while autophagy inhibition may impede recovery. However, some findings sug-

gest that suppressing autophagy 48 hours post-SCI can improve motor function recovery, whereas its stimulation does not yield significant benefits [33, 34]. In this study, we further explored whether SGB modulates the autophagy pathway in spinal neurons post-SCI. LC3 and p62 were selected as primary indicators to detect autophagy, as both play critical roles in the autophagic process. An increased LC3-II/LC3-I ratio signifies the initiation of autophagy, whereas elevated p62 levels suggest impaired autophagic degradation and disrupted autophagic flux. Our results demonstrated that on days 1, 3, and 7 post-injury, the SCI group exhibited significantly higher levels of p62 and LC3-II/LC3-I in the spinal cord, suggesting that SCI induces autophagy. However, the concurrent increase in p62 levels indicates that injury not only disrupts autophagic flux but also impairs autophagic degradation, consistent with previous studies showing that NP models can lead to autophagic flux obstruction and autophagy dysfunction [35]. Following SGB treatment in SCI rats, a significant increase in the LC3-II/LC3-I ratio in the spinal cord was observed on day 3 post-injury, surpassing levels recorded on days 1 and 7, along with a concurrent decrease in p62 expression. This suggests that SGB enhanced autophagy in the spinal cord of rats post-SCI and facilitated autophagic flux clearance. Additionally, electron microscopy findings revealed increased autophagosome levels in spinal cord tissues, corroborating the Western blot results. Together, these findings imply that SGB alleviate NP by promoting autophagy in spinal cord neurons.

Conclusions

Our findings indicate that SCI induces motor dysfunction and a reduced pain threshold in rats. Furthermore, SCI significantly elevates inflammatory cytokine levels, such as IL-1 β , and enhances apoptosis and autophagy while impairing autophagic flux. Stellate ganglion block (SGB) effectively alleviates neuropathic pain behaviors, reduces inflammatory factor levels in the spinal cord, mitigates spinal cord apoptosis and injury, and enhances both autophagy and autophagic flux post-SCI. These findings provide new insights into the pathogenesis of neuropathic pain following spinal cord injury and suggest that SGB may serve as a potential therapeutic strategy.

Acknowledgements

The present study was supported by funds from the Guizhou Province Science and Technology Plan Project [Guizhou combination-Basics [2023] Key 044] and the Guizhou Province Science and Technology Plan Project [Qiankehe Foundation-ZK [2023] General 389] and the Guizhou Province Science and Technology Plan Project [Grants number: Qiankehe Foundation-ZK [2024] Key 036] and the National Natural Science Foundation of China Cultivation Project of Guizhou Medical University [Item number: 21NSFSP09].

Disclosure of conflict of interest

None.

Address correspondence to: Jing Yao and Zhongjie Zhang, Department of Pain, The Affiliated Hospital of Guizhou Medical University, No. 28, Guiyi Street, Liuguangmen, Guiyang 550004, Guizhou, China. E-mail: gyfyyaoj@163.com (JY); 250416722@qq.com (ZJZ)

References

- [1] Cofano F, Boido M, Monticelli M, Zenga F, Ducati A, Vercelli A and Garbossa D. Mesenchymal stem cells for spinal cord injury: current options, limitations, and future of cell therapy. *Int J Mol Sci* 2019; 20: 2698.
- [2] Kang J, Cho SS, Kim HY, Lee BH, Cho HJ and Gwak YS. Regional hyperexcitability and chronic neuropathic pain following spinal cord injury. *Cell Mol Neurobiol* 2020; 40: 861-878.
- [3] Hu X, Xu W, Ren Y, Wang Z, He X, Huang R, Ma B, Zhao J, Zhu R and Cheng L. Spinal cord injury: molecular mechanisms and therapeutic interventions. *Signal Transduct Target Ther* 2023; 8: 245.
- [4] Sterner RC and Sterner RM. Immune response following traumatic spinal cord injury: pathophysiology and therapies. *Front Immunol* 2023; 13: 1084101.
- [5] Widerström-Noga E. Neuropathic pain and spinal cord injury: management, phenotypes, and biomarkers. *Drugs* 2023; 83: 1001-1025.
- [6] Cohen SP, Vase L and Hooten WM. Chronic pain: an update on burden, best practices, and new advances. *Lancet* 2021; 397: 2082-2097.
- [7] Knowles CH and Cohen RC. Chronic anal pain: a review of causes, diagnosis, and treatment. *Cleve Clin J Med* 2022; 89: 336-343.
- [8] Alizadeh A, Dyck SM and Karimi-Abdolrezaee S. Traumatic spinal cord injury: an overview of pathophysiology, models and acute injury mechanisms. *Front Neurol* 2019; 10: 282.
- [9] Hu N, Wu Y, Chen BZ, Han JF and Zhou MT. Protective effect of stellate ganglion block on delayed cerebral vasospasm in an experimental rat model of subarachnoid hemorrhage. *Brain Res* 2014; 1585: 63-71.
- [10] Zille M, Farr TD, Keep RF, Römer C, Xi G and Boltze J. Novel targets, treatments, and advanced models for intracerebral haemorrhage. *EBioMedicine* 2022; 76: 103880.
- [11] Datta R, Agrawal J, Sharma A, Rathore VS and Datta S. A study of the efficacy of stellate ganglion blocks in complex regional pain syndromes of the upper body. *J Anaesthesiol Clin Pharmacol* 2017; 33: 534-540.
- [12] Wen S, Chen L, Wang TH, Dong L, Zhu ZQ and Xiong LL. The efficacy of ultrasound-guided stellate ganglion block in alleviating postoperative pain and ventricular arrhythmias and its application prospects. *Neurol Sci* 2021; 42: 3121-3133.
- [13] Basso DM, Fisher LC, Anderson AJ, Jakeman LB, McTigue DM and Popovich PG. Basso mouse scale for locomotion detects differences in recovery after spinal cord injury in five common mouse strains. *J Neurotrauma* 2006; 23: 635-659.
- [14] Xue MT, Sheng WJ, Song X, Shi YJ, Geng ZJ, Shen L, Wang R, Lü HZ and Hu JG. Atractylenolide III ameliorates spinal cord injury in rats by modulating microglial/macrophage polarization. *CNS Neurosci Ther* 2022; 28: 1059-1071.
- [15] Zhao L, Tao X, Wang Q, Yu X and Dong D. Diosmetin alleviates neuropathic pain by regulating the Keap1/Nrf2/NF- κ B signaling pathway. *Biomed Pharmacother* 2024; 170: 116067.
- [16] Ushida T, Katayama Y, Hiasa Y, Nishihara M, Tajima F, Katoh S, Tanaka H, Maeda T, Furusawa K, Richardson M, Kakehi Y, Kikumori K and Kuroha M. Mirogabalin for central neuropathic pain after spinal cord injury: a randomized, double-blind, placebo-controlled, phase 3 study in Asia. *Neurology* 2023; 100: e1193-e1206.
- [17] Yang L, Blumbergs PC, Jones NR, Manavis J, Sarvestani GT and Ghabriel MN. Early expression and cellular localization of proinflammatory cytokines interleukin-1 β , interleukin-6, and tumor necrosis factor- α in human traumatic spinal cord injury. *Spine (Phila Pa 1976)* 2004; 29: 966-971.
- [18] Green-Fulgham SM, Ball JB, Kwilas AJ, Harland ME, Frank MG, Dragavon JM, Grace PM and Watkins LR. Interleukin-1 β and inflammatory expression in spinal cord following chronic constriction injury in male and female rats. *Brain Behav Immun* 2024; 115: 157-168.

- [19] Szok D, Tajti J, Nyári A and Vécsei L. Therapeutic approaches for peripheral and central neuropathic pain. *Behav Neurol* 2019; 2019: 8685954.
- [20] Finnerup NB, Attal N, Haroutounian S, McNicol E, Baron R, Dworkin RH, Gilron I, Haanpää M, Hansson P, Jensen TS, Kamerman PR, Lund K, Moore A, Raja SN, Rice AS, Rowbotham M, Sena E, Siddall P, Smith BH and Wallace M. Pharmacotherapy for neuropathic pain in adults: a systematic review and meta-analysis. *Lancet Neurol* 2015; 14: 162-173.
- [21] Eller OC, Willits AB, Young EE and Baumbauer KM. Pharmacological and non-pharmacological therapeutic interventions for the treatment of spinal cord injury-induced pain. *Front Pain Res (Lausanne)* 2022; 3: 991736.
- [22] Almeida C, Monteiro-Soares M and Fernandes Â. Should non-pharmacological and non-surgical interventions be used to manage neuropathic pain in adults with spinal cord injury? - A systematic review. *J Pain* 2022; 23: 1510-1529.
- [23] Mulvaney SW, Lynch JH and Kotwal RS. Clinical guidelines for stellate ganglion block to treat anxiety associated with posttraumatic stress disorder. *J Spec Oper Med* 2015; 15: 79-85.
- [24] Johnston CH, Whittaker AL, Franklin SH and Hutchinson MR. The neuroimmune interface and chronic pain through the lens of production animals. *Front Neurosci* 2022; 16: 887042.
- [25] Borovikova LV, Ivanova S, Zhang M, Yang H, Botchkina GI, Watkins LR, Wang H, Abumrad N, Eaton JW and Tracey KJ. Vagus nerve stimulation attenuates the systemic inflammatory response to endotoxin. *Nature* 2000; 405: 458-462.
- [26] Zhong ZX, Feng SS, Chen SZ, Chen ZM and Chen XW. Inhibition of MSK1 promotes inflammation and apoptosis and inhibits functional recovery after spinal cord injury. *J Mol Neurosci* 2019; 68: 191-203.
- [27] Klionsky DJ, Petroni G, Amaravadi RK, Baehrecke EH, Ballabio A, Boya P, Bravo-San Pedro JM, Cadwell K, Cecconi F, Choi AMK, Choi ME, Chu CT, Codogno P, Colombo MI, Cuervo AM, Deretic V, Dikic I, Elazar Z, Eskelinen EL, Fimia GM, Gewirtz DA, Green DR, Hansen M, Jäättelä M, Johansen T, Juhász G, Karantza V, Kraft C, Kroemer G, Ktistakis NT, Kumar S, Lopez-Otin C, Macleod KF, Madeo F, Martinez J, Meléndez A, Mizushima N, Münz C, Penninger JM, Perera RM, Piacentini M, Reggiori F, Rubinsztein DC, Ryan KM, Sadoshima J, Santambrogio L, Scorrano L, Simon HU, Simon AK, Simonsen A, Stolz A, Tavernarakis N, Tooze SA, Yoshimori T, Yuan J, Yue Z, Zhong Q, Galluzzi L and Pietrocola F. Autophagy in major human diseases. *EMBO J* 2021; 40: e108863.
- [28] Levine B and Kroemer G. Biological functions of autophagy genes: a disease perspective. *Cell* 2019; 176: 11-42.
- [29] Leonardi L, Sibénil S, Alifano M, Cremer I and Joubert PE. Autophagy modulation by viral infections influences tumor development. *Front Oncol* 2021; 11: 743780.
- [30] Jiang X, Huang Y, Liang X, Jiang F, He Y, Li T, Xu G, Zhao H, Yang W, Jiang G, Su Z, Jiang L and Liu L. Metastatic prostate cancer-associated P62 inhibits autophagy flux and promotes epithelial to mesenchymal transition by sustaining the level of HDAC6. *Prostate* 2018; 78: 426-434.
- [31] Li Y, Lei Z, Ritzel RM, He J, Li H, Choi HMC, Lipinski MM and Wu J. Impairment of autophagy after spinal cord injury potentiates neuroinflammation and motor function deficit in mice. *Theranostics* 2022; 12: 5364-5388.
- [32] Sakai K, Fukuda T and Iwadate K. Immunohistochemical analysis of the ubiquitin proteasome system and autophagy lysosome system induced after traumatic intracranial injury: association with time between the injury and death. *Am J Forensic Med Pathol* 2014; 35: 38-44.
- [33] Zhang D, Yuan Y, Zhu J, Zhu D, Li C, Cui W, Wang L, Ma S, Duan S and Liu B. Insulin-like growth factor 1 promotes neurological functional recovery after spinal cord injury through inhibition of autophagy via the PI3K/Akt/mTOR signaling pathway. *Exp Ther Med* 2021; 22: 1265.
- [34] Fang B, Li XQ, Bao NR, Tan WF, Chen FS, Pi XL, Zhang Y and Ma H. Role of autophagy in the bimodal stage after spinal cord ischemia reperfusion injury in rats. *Neuroscience* 2016; 328: 107-116.
- [35] Liu X, Zhu M, Ju Y, Li A and Sun X. Autophagy dysfunction in neuropathic pain. *Neuropeptides* 2019; 75: 41-48.